Copper nanoparticles have negligible direct antibacterial impact

NanoImpact 17 (2020) 100192

Contents lists available at ScienceDirect

NanoImpact

journal homepage: www.elsevier.com/locate/nanoimpact

Research paper

Copper nanoparticles have negligible direct antibacterial impact

Carlos A.P. Bastos[a,*], Nuno Faria[a], John Wills[a], Per Malmberg[b], Nathalie Scheers[c], Paul Rees[d,e], Jonathan J. Powell[a,*]

[a] Biomineral Research Group, Department of Veterinary Medicine, University of Cambridge, Madingley Road, Cambridge CB3 0ES, UK
[b] Department of Chemistry and Chemical Engineering, Chalmers University of Technology, Gothenburg, Sweden
[c] Department of Biology and Biological Engineering, Chalmers University of Technology, Gothenburg, Sweden
[d] Centre for Nanohealth, Swansea University College of Engineering, Fabian Way, Crymlyn Burrows, Swansea SA1 8EN, UK
[e] Broad Institute of MIT and Harvard, 415 Main Street, Cambridge, MA 02142, United States

ARTICLE INFO

Editor: Jamie Lead

Keywords:
Copper
Antimicrobial
Nanoparticle
Nano
Antibacterial

ABSTRACT

Introduction: Soluble copper that can be acquired by bacteria is toxic and therefore antimicrobial. Whether nanostructured copper materials, in either disperse or agglomerated form, have antimicrobial impact, aside from that of their dissolution products, is not clear and was herein addressed.

Methods: We took five nanostructured copper materials, two metallic, and three oxo-hydroxides with one of these being silicate-substituted. Four agglomerated in the bacterial growth media whilst the silicate-substituted material remained disperse and small (6.5 nm diameter). Antibacterial activity against *E. coli* was assessed with copper phase distribution measured over time. Using the dose of soluble copper, and benchmark dose non-linear regression modelling, we determined how well this phase predicted antimicrobial activity. Finally, we used Time-of-Flight Secondary Ion Mass Spectrometry (ToF-SIMS) analysis to investigate whether membrane adhesion effects by copper were plausible or if intracellular uptake most likely explained the bacterial impact of copper.

Results: Comparison over time of antimicrobial activity against particulate or soluble phases of the aquated materials clearly demonstrated that soluble copper but not particulate forms were associated with inhibition of bacterial growth. Indeed, the benchmark dose modelling showed the soluble dose required to cause a 50% reduction in *E. coli* growth was strongly clustered – for all particle formulations – at 14.5 mg/L (10–19 mg/L 90% confidence interval). By comparison, total copper levels associated with the same reduction in viability varied widely (45–549 mg/L). Finally, in favour of this soluble product dominance in terms of antimicrobial activity, copper had low association with bacterial membrane (something both soluble and particulate materials could do) but showed high intra-bacterial levels (something only soluble copper could do).

Conclusion: Taken together our data show that it is the uptake of soluble but not particulate copper, and the intracellular loading not just contact and membrane association, that drives copper toxicity to bacteria. Therapeutic strategies for novel antimicrobial copper compounds should consider these findings.

1. Introduction

Nanostructuring of materials may lead to changes in physicochemical properties, beyond size differences, when compared to the bulk material counterparts (Pfeiffer et al., 2014; Santos et al., 2018). Whilst this can create novel applications and commercial opportunities, it has also brought about concerns over exposure and safety for humans, other animals and the environment (Chen et al., 2017; McClements and Xiao, 2017).

Copper has broad-spectrum antimicrobial properties (Ingle et al., 2014; Lemire et al., 2013). This could be exploited for therapeutic benefit but, equally, exposures could yield undesirable activity against symbiotic bacteria in the environment, the skin or the intestine (*i.e.* the microbiome). So understanding copper-bacteria interaction is

Abbreviations: BMD, benchmark dose; CuNPs, elemental copper nanoparticles; CuO NPs, copper oxide nanoparticles; CuSi NPs, silicate-stabilised copper hydroxide nanoparticles; DLS, Dynamic Light Scattering; *E. coli*, *Escherichia coli*; EFSA, European Food Safety Authority; FT-IR, Fourier Transform – Infra Red; HMM, Heavy Metal MOPS medium; ICP-OES, Inductively Coupled Plasma – Optical Emission Spectrometry; MOPS, 3-(N-morpholino)propanesulfonic acid; OD, optical density; SLS, static light scattering; TBS, Tryptic Soy Broth medium; ToF-SIMS, Time-of-Flight Secondary Ion Mass Spectrometry; UHP, ultra high purity

* Corresponding authors.
E-mail addresses: capb2@cam.ac.uk (C.A.P. Bastos), jjp37@cam.ac.uk (J.J. Powell).

https://doi.org/10.1016/j.impact.2019.100192
Received 9 August 2019; Received in revised form 24 October 2019; Accepted 4 November 2019
Available online 20 November 2019

important (Lemire et al., 2013). How much the nanostructuring of copper-based materials governs their antimicrobial properties is not fully understood. Certainly this nanostructuring strategy may be used to tailor 'slow release' properties for copper ions or to allow stable aqueous formulations of copper at high concentrations without issues with hydrolysis and precipitation (Bastos et al., 2018; Herrmann and Bucksch, 2015; Paulson and Kester, 1980). However, this does not address whether particles themselves have a microbial impact beyond or in addition to released soluble copper. On the one hand, by comparison to silver (Xiu et al., 2012), one might assume that it is only soluble copper, not particles, that are antimicrobial. On the other hand, increased activities of copper-based nanoparticles, above and beyond just copper ion content, have been indicated (Chen et al., 2019; Raffi et al., 2010; Sarkar et al., 2012). Indeed, the issue of whether nanoparticles *per se* have specific activity against bacteria, remains unclear but important. For example, the European Food Safety Authority (EFSA) requests that, for new oral nanoparticles that are relevant to food, tests are carried out in terms of microbiome effects for safety assessment (EFSA, 2018).

In trying to determine whether copper-based particles, or the copper ions that they release in an aqueous environment, are responsible for antimicrobial activity, a number of aspects must be carefully considered. Firstly, in standard bacterial assays, total exposure to particulate or soluble (solubilised) copper will be determined by an interaction between time and rates of particle dissolution. Secondly, the chemistry of copper is complicated. At typical biological (near–neutral) pHs, particles may form when 'soluble' salts are added to a solution phase, due to oxo-hydroxide formation, polymerisation, cross-linking and precipitation (Paulson and Kester, 1980; Zhang and Richardson, 2016). Finally, particles, whether inadvertently formed or specifically added to a fluid phase, may agglomerate and/or aggregate. As such, studies investigating exactly what bacteria experience in terms of exposure to copper-based particles, and thus what chemical form is active, are lacking (Ingle et al., 2014).

Here, we took advantage of the differential solution behaviour of various formulations of copper-based particles and we measured their low molecular weight (soluble), nano and agglomerated fractions over time in bacterial culture medium alongside their antimicrobial impact against *Escherichia coli*, a laboratory standard for clinically relevant gram-negative bacteria which are increasingly associated with antibiotic resistant infections (Cassini et al., 2019). We then used benchmark dose modelling to determine the variability in effector activity of the different phases of each particle type. Finally, we used ToF SIMS analysis to investigate whether membrane adhesion effects by copper were plausible, or, if intracellular uptake most likely explained the bacterial impact of copper.

2. Materials and methods

2.1. Preparation of copper stocks

All reagents were purchased from Sigma Aldrich and used as received, unless otherwise detailed. Copper nanopowders were purchased from Sigma Aldrich or Alfa Aesar (Table 1). Stock solutions were prepared using ultra high purity (UHP) water (reverse osmosis purification; 18.2 ΩM/cm). Dispersions of copper oxide nanoparticles (CuO NPs A) were prepared from commercial powders (Sigma 544868) that were reported as free of impurities and with a primary particle size of 34 nm (Moschini et al., 2013). These have been previously investigated as antimicrobial agents (Aruoja et al., 2009; Bastos et al., 2018). The stocks were prepared at 20 mM copper by dispersing the powder in water with vigorous agitation. The same protocol was repeated for copper oxide nanoparticles Alfa Aesar 44663 (termed here as CuO NPs B). Elemental copper nanoparticles, Sigma 774081 (termed here as CuNPs A) and Sigma 774111 (termed here as CuNPs B), were maintained in an oxygen-free environment before use and were dispersed in UHP water (20 mM copper) that had been flushed with nitrogen gas to reduce oxygen exposure. Their purity was confirmed *via* Fourier Transform – Infrared (FT-IR) spectroscopy and by determining that the particles were 97% copper (Appendix A). Finally, silicate-stabilised copper hydroxide nanoparticles (CuSi NPs) were synthesised by mixing equal volumes of 400 mM sodium silicate (*ca.* pH 12) and 40 mM copper chloride, which resulted in formation of blue-coloured aggregates. 5 M NaOH was then added, under agitation to adjust the suspension to pH 12 ± 0.2 and the mixture was kept under stirring until full colloidal dispersion was observed (*ca.* after 24 h).

2.2. Particle characterisation in liquid suspensions

2.2.1. Particle sizing measurements

Following Initial inspection of commercial copper-based particles dispersed in bacterial medium (Heavy Metals MOPS medium here termed as HMM; full description in Appendix B), fast sedimentation indicated that these were not nano-sized when suspended in aqueous media. Therefore, static light scattering (SLS) was used to formally determine the *de facto* particle size distribution of commercial copper nanoparticles using a Mastersizer 2000 fitted with a Hydro 2000 μP Micro Precision sample dispersion unit (Malvern Instruments Ltd., UK). For each measurement, *ca.* 787 μL of each 20 mM copper stock was added directly to the 20 mL dispersion cell unit containing HMM. The resulting dispersion (50 mg/L copper in HMM) was run at 1000 rpm and three consecutive measurement cycles were carried out for each material with the settings described in Appendix C.

Dynamic Light Scattering (DLS) was used to determine the hydrodynamic particle size distribution by of the CuSi NPs suspension (20 mM copper). The measurements were performed on a Zetasizer NanoZS (Malvern Instruments Ltd., UK) using a 1 mL disposable cuvette and a temperature of 25 ± 2 °C (n = 3). Detailed settings for the analysis can be found in Appendix C.

2.2.2. Size categorisation in bacterial medium

To ensure that the light scatter signal from aquated microparticles, above, was not masking a significant nano-fraction (Malvern Instruments, 2015), we also carried out size categorisation by ultrafiltration and centrifugation followed by elemental analysis. Copper-based particle stocks with starting concentration of 20 mM copper were diluted in bacterial medium – Heavy Metal MOPS medium (HMM) – to 50 mg/L (*ca.* 0.8 mM). Three aliquots of each stock were collected to determine: a) the total copper content (Cu_{Total}), b) copper in the supernatant after centrifugation at 16000*g* for 5 min ($Cu_{Supernatant}$), and c)

Table 1
Properties of commercial copper nanopowders as described by suppliers.

Reference	Label	Composition	Molecular weight	Primary particle size
Sigma 544868	CuO NPs A	Copper oxide (CuO)	79.545	< 50 nm 10–50 nm (Moschini et al., 2013)
Alfa Aesar 44663	CuO NPs B	Copper oxide (CuO)	79.545	30–50 nm
Sigma 774081	Cu NPs A	Elemental Cu (Cu^0)	63.546	25 nm
Sigma 774111	Cu NPs B	Elemental Cu (Cu^0)	63.546	40–60 nm

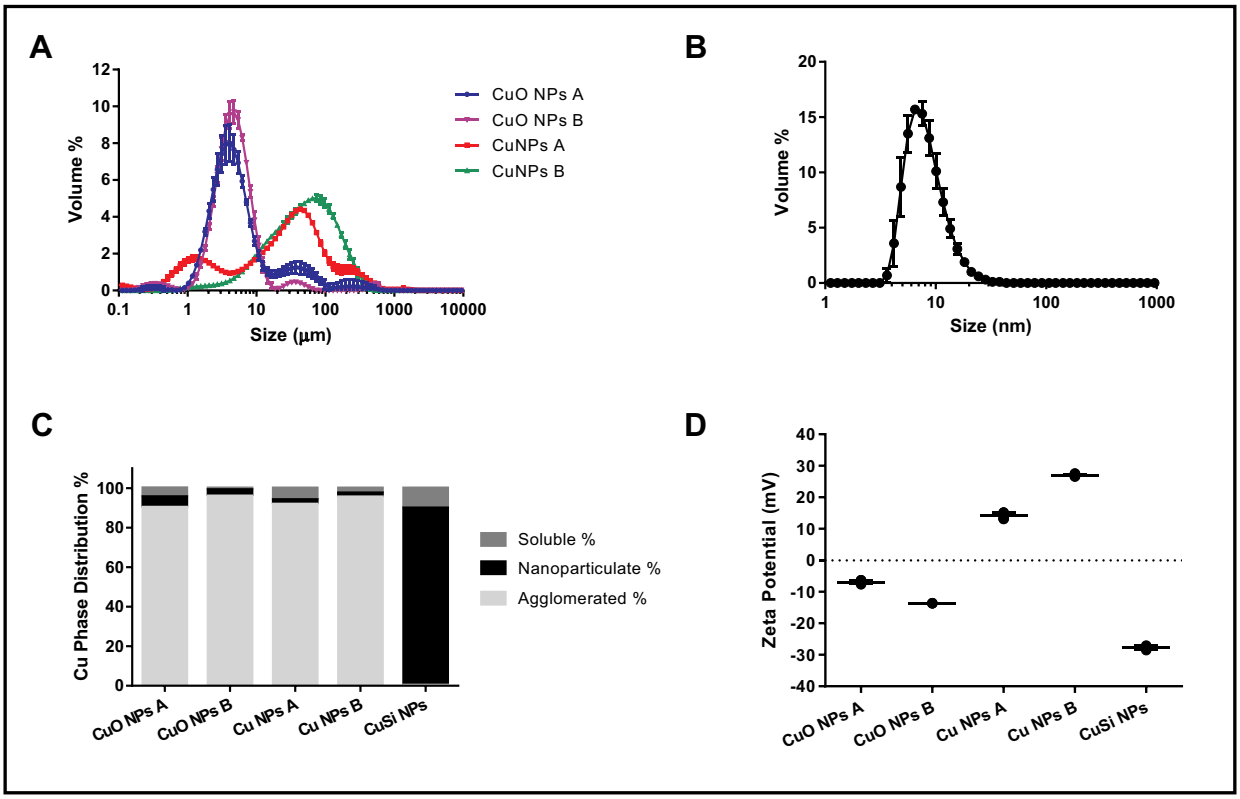

Fig. 1. Particle characterisation in stock solutions and bacterial medium. (A) Particle size distribution of commercial copper nanoparticles in bacterial medium (HMM) at 50 mg/L copper obtained by static light scattering. (B) Particle size distribution of CuSi NPs in its original stock at 20 mM in water. (C) Copper phase distribution of nanoparticle in bacterial medium (HMM) at 50 mg/L Cu. (D) Zeta potential of copper nanoparticles in their corresponding stocks at 20 mM copper.

soluble copper content, after filtration with a 3KDa centrifuge filter (Sartorius Vivaspin 500 VS0192) for 5 min at 16000 g (Cu_{3KDa}). Following size differentiation, aliquots were diluted down to 20 mg/L in 5% HNO_3 (v/v) or lower and kept for at least 24 h prior to analysis to ensure full dissolution. Copper concentration was then determined by inductively coupled plasma-optical emission spectroscopy at 324.754 nm (ICP-OES; Jobin Yvon 2000, Horiba, UK) using matrix-matched calibration standards (0.1 to 20 mg/L). Finally, the different fractions were calculated as per equations below:

$$Agglomerated\ (\%) = \frac{Cu_{Total} - Cu_{supernatant}}{Cu_{Total}} \times 100$$

$$Soluble\ (\%) = \frac{Cu_{3Kda}}{Cu_{Total}} \times 100$$

$$Nanoparticulate\ (\%) = 100 - (Soluble\ (\%) + \text{Agglomerated}\ (\%))$$

2.2.3. Soluble and particulate content in bacterial medium

20 mM coper stocks were diluted in HMM to 12.5, 25 and 50 mg/L copper and incubated overtime at 30 °C under constant agitation (80 rpm) in an Infors HT Minitron incubator. Samples were collected overtime for elemental analysis as described in 2.2.2. Soluble copper content was defined as low molecular weight copper that passed through a 3KDa filter (Cu_{3kDa}), whilst the remaining copper was considered particulate ($Cu_{Total} - Cu_{3kDa}$).

2.2.4. Zeta Potential Measurements

The zeta potential of copper particles stocks was determined by Laser Doppler Micro-electrophoresis (Zetasizer NanoZS, Malvern Instruments Ltd., UK) using disposable folded capillary cells (DTS1070) and assuming a dielectric constant of 78.5 and a viscosity of 0.89 cP. Cells were carefully filled with copper particle suspensions using a syringe to avoid air bubbles, and analysis carried out as per standard guidelines of the instrument manufacturer.

2.3. Antibacterial activity of copper materials

Antibacterial activity of copper materials was assessed using a broth microdilution assay which is a standard approach for antimicrobial susceptibility testing in solution (ESCMID, 2003; Reller et al., 2009). The assays were carried out using starting bacterial loads of *ca.* 10^6 CFU/mL, which is the minimum quantifiable by optical density (OD595nm = 0.05–0.1) allowing bacterial growth to be followed over time and, therefore, copper effects to be assayed quantitatively. Copper speciation and bacterial growth were followed over time. For this, *Escherichia coli* (NCTC11100) cultures were grown in HMM (full composition in Appendix B), a defined media with low metal chelation ability (LaRossa et al., 1995), which was supplemented with 0.4% glucose and 0.1% casein acid hydrolysate, and pH adjusted to 7.2 ± 0.2. Overnight bacterial cultures were prepared at 30 °C in HMM under constant agitation (80 rpm) in an Infors HT Minitron incubator. A turbidimetric assay was used to follow bacterial growth over time by measuring optical density (OD) at 595 nm using a Multiskan RC 351 Labsystem plate reader. 20 mM (*ca.* 1.27 g/L) copper particle stocks were pre-diluted in HMM and then mixed with *E. coli* suspensions that, as noted above, were diluted to an optical density of 0.05–0.1 OD reading (*ca.* 10^6 CFU/mL). Final copper concentrations were 0, 12.5, 25 and 50 mg/L copper. These were chosen to be measurably toxic to bacteria whilst allowing for observations on how variance in particulate and soluble copper concentrations impacted growth inhibition. Bacterial cells and particles were incubated for 8 h at 30 °C under agitation (80 rpm) and OD measurements were obtained at different time points. Background, *i.e.* OD of bacteria-free media, was subtracted for both control (OD for media only) and for copper (OD for media plus copper material) and

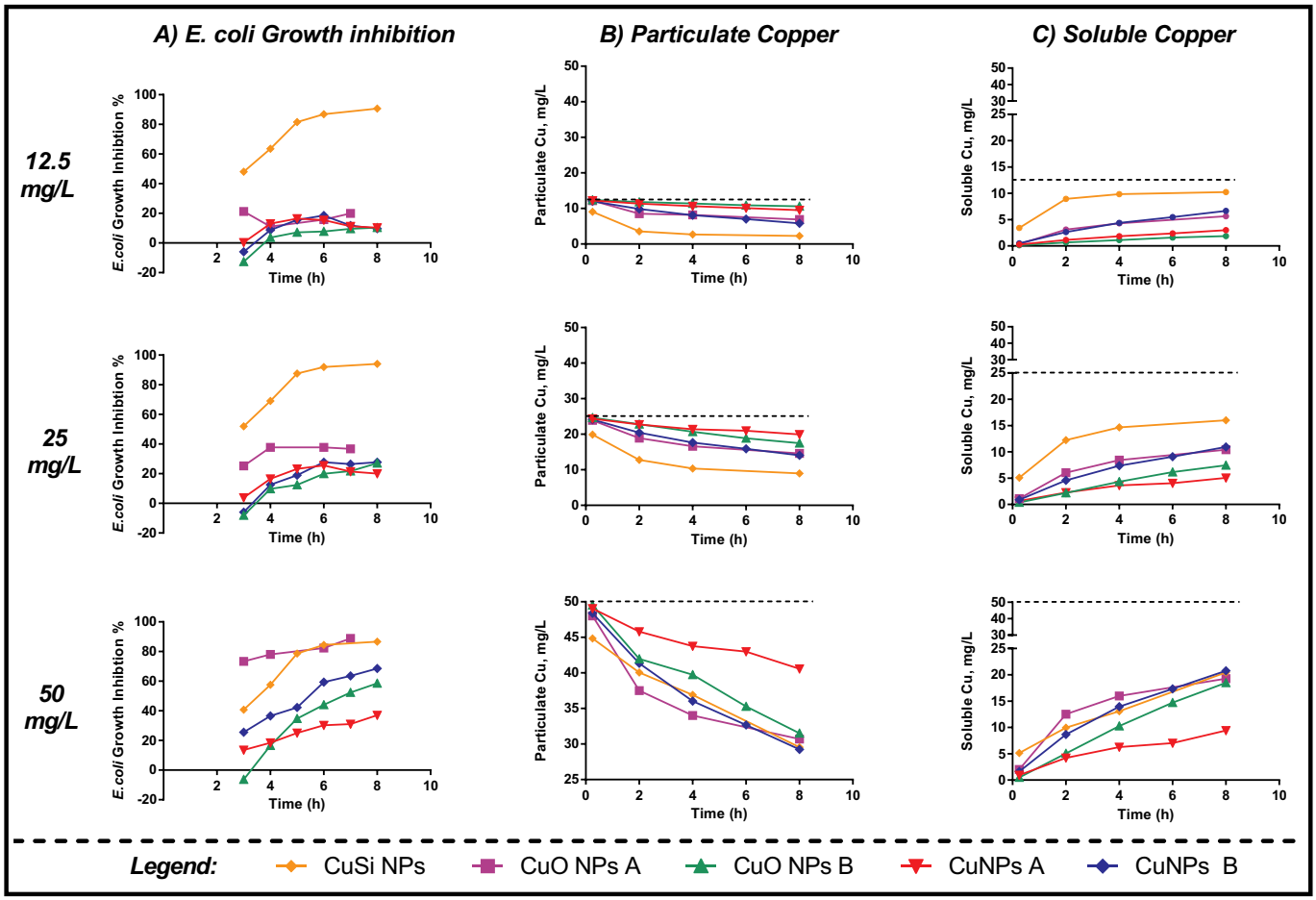

Fig. 2. Antimicrobial activity and phase distribution of the materials in bacterial medium.
(A) *E. coli* growth inhibition (%) as a function of time upon incubation with copper nanoparticles at 12.5 mg/L (top), 25 mg/L (middle) and 50 mg/L (bottom). (B) Particulate copper in bacterial medium overtime and (C) soluble copper released in bacterial medium over time upon incubation with copper nanoparticles at 12.5 mg/L (top), 25 mg/L (middle) and 50 mg/L (bottom).

Bacterial growth inhibition over time was determined by comparing with OD readings for copper treated against control, as per equation below:

$$\text{Growth Inhibition}\% = \left(\frac{OD\ Control - OD\ Copper\ Treated}{OD\ Control}\right) \times 100$$

2.4. Benchmark response modelling

Benchmark dose (BMD), *i.e.* non-linear regression analysis, was conducted using the combined BMD-covariate approach described extensively in previous work (Wills et al., 2015, 2016, 2017). Analyses were carried out the R computing environment using the freely available PROAST package (http://www.proast.nl). The bacterial viability dose-response data were analysed using a nested family of four-parameter exponential models recommended for the analysis of continuous toxicity data by the EFSA (EFSA, 2009, 2017). In each analysis, combined dose response data for either the total dose of copper (*i.e.*, the dose-time product) or the released dose of soluble copper were analysed using the factor discriminating the subgroups (*i.e.*, copper-based nanoparticle type) as a covariate. Models were iteratively fitted to the data with more complex models with increasing numbers of covariate-dependent parameters only accepted if the difference in log-likelihood exceeded $P < 0.05$. This approach allowed determination of which model parameters needed to be estimated for each subgroup, and which parameters could be considered constants across the combined data. Interpolation from the fitted model allowed estimation of the dose (*i.e.*, the BMD) that could be expected to cause the benchmark response (set here at a 50% reduction in bacterial viability) for each of the particle formulations.

2.5. TOF-SIMS analysis

A 40 mM copper chloride solution was diluted to 500 mg/L (*ca.* 7.9 mM) in HMM and this stock was then further diluted to 12.5 mg/L copper in an *E. coli* (DH_5 alpha) culture in the stationary phase (precultured in Tryptic Soy Broth medium (TBS) and added in the exponential phase to HMM overnight cultures (37 °C, 200 rpm; 1.9 cm orbit; Max 4000 Barnstead Lab-line)). Copper and bacteria were incubated at room temperature for 2 h with no agitation. This culture was subsequently centrifuged at 1500 rpm (250g; Heraeus multifuge) for 5 min and the supernatant containing the medium and free copper was discarded. The remaining cell pellet was resuspended to the original volume in UHP water. A sample droplet was mounted on a silicon wafer, heat-dried, and analysed by TOF-SIMS.

ToF-SIMS imaging and depth profiling was performed using a TOF.SIMS V (ION-TOF, GmbH) using a 25 keV bismuth liquid metal ion gun as a primary ion source and a 10 KeV C_{60} ion source as a sputter source. The delayed extraction mode was used for imaging with an approximate lateral resolution of 400 nm at a mass resolution of approx. 3500 at m/z 58. The pulsed primary ion current of the Bi_3^+ ion used was 0.2 pA. The total primary ion dose density was 1×10^{11} ions/cm^2 and therefore below the static limit. The SurfaceLab 6 software (v. 6.6, ION-TOF GmbH) was used for all processing of images and depth profiles. The mass spectra were calibrated internally to signals of $[CH_3]^+$, $[C_5H_{12}N]^+$, and $[C_5H_{15}PNO_4]^+$.

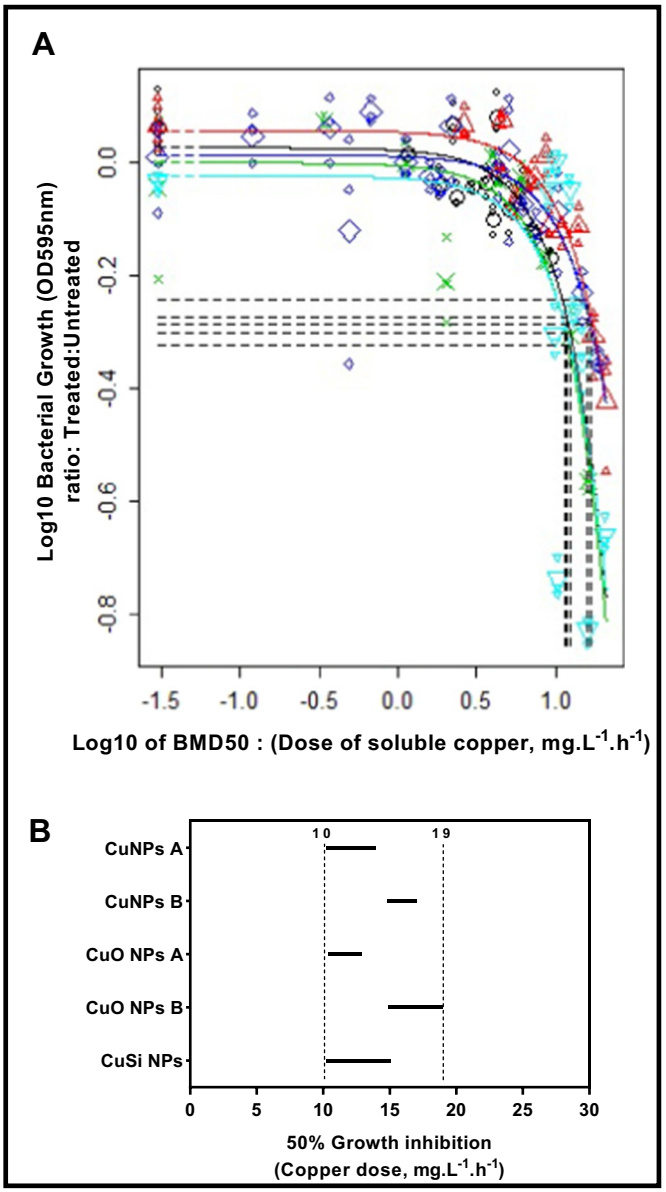

Fig. 3. Correlation between bacterial growth inhibition and total soluble copper released from the particles. (A) Benchmark dose non-linear regression modelling to compare the effect of released soluble copper on bacterial growth inhibition. (B) 90% confidence intervals from each analysis, showing for each particle formulation the dose required to elicit a 50% reduction in bacterial growth. The intervals for soluble copper converge into a narrow range, unlike for total copper that shows poor correlation across formulations, suggesting ion release drives the inhibition effect observed.

Depth profiling was performed in the non-interlaced mode (2 shots per pixel, 1 frame per sputter cycle of 1 s with a 0.5 s pause) using $C60^{++}$ ions at a current of 0.15 nA. Craters were sputtered ranging from 150 × 150 μm^2 to 300 × 300 μm^2 whilst analysing areas of 50 × 50 μm^2 to 150 × 150 μm^2 using the primary ions. The ratio between the analysed area and the sputtered area was > 1.5. The total C60 dose in the experiments ranged from 4.9 × 10^{13} ions/cm^2 to 5.8 × 10^{14} ions/cm^2.

3. Results

In the HMM bacterial medium, the commercially available nanoparticles were chiefly polydisperse micron-sized agglomerates as determined by static light scattering measurements (Fig. 1A). The copper oxides were mostly 1–10 μm in diameter and the copper metal particles were larger (10–1000 μm). In contrast, the in-house-synthesised, silicate-substituted copper oxo-hydroxides (termed CuSi NPs) had a modal diameter of 6.5 nm and almost all were 4–20 nm in size (Fig. 1B). Size differentiation experiments, based on filtration and centrifugation, confirmed these findings with the aquated commercial particles dominated by agglomerated material and the in-house-synthesised particles dominated by a small nano fraction (Fig. 1C). As expected, the copper metal particles were positively-charged in the HMM medium and the copper oxides were negatively charged (Fig. 1D) with the aquated nanoparticles (*i.e.* the CuSi NPs) showing a large enough negative zeta potential (−27 ± 1 mV; Fig. 1D) for stable suspension in aqueous media (Bhattacharjee, 2016).

When the particles were aquated in the *E. coli*-containing bacterial medium, it was apparent that, except at the highest levels of exposure (50 mg/L copper), the aquated nanoparticulate material had much greater antimicrobial activity than the large particle material, during the 8 h of experimentation (Fig. 2A). Moreover, the particulate fraction, whether nano (CuSi NPs) or larger (other materials) or whether positively or negatively charged, appeared inversely related to bacterial growth inhibition (Fig. 2B). Indeed, as therefore expected, the soluble fraction of copper appeared clearly related to inhibition of *E. coli* growth, over time, for all materials (Fig. 2C). Notwithstanding, the interaction between time and solubility did not facilitate intuitive understanding of just how well soluble copper concentration might explain antimicrobial activity. To enable this, we modelled the effects on bacterial viability over time using benchmark dose non-linear regression modelling. Firstly, we confirmed that exposure to total copper in suspension was a very poor predictor of antimicrobial potency as would be expected for combined soluble and particulate copper (Appendix D). In contrast, the results for soluble copper converged across all formulations tested to very similar benchmark dose levels (Fig. 3). Indeed, when the dose required to cause a 50% reduction in *E. coli* viability was compared, the total copper data showed an order of magnitude variance (45–549 mg/L Cu) between particle types (Appendix D). Contrastingly, the dose of soluble copper required was tightly clustered for all formulations around 14.5 mg/L with the 90% confidence interval across all particle types spanning a range of just 10–19 mg/L (Fig. 3).

Collectively, these data strongly imply that soluble, but not particulate copper levels whether nano or larger, achieved by hydrated copper-containing particles, determine a material's antimicrobial activity. Finally, therefore, to confirm this we considered the intracellular (*i.e.* intra-bacterial) levels of copper *versus* that of the outer membrane following soluble copper exposure. We reasoned that a non-contact effect would favour intracellular copper localisation rather than membrane localisation, because the latter could have been achieved in the studies above with particles, whereas the former could not have been achieved with particle surfaces since bacteria have rigid membranes and no ability to internalise particles (Santos et al., 2018). We did not use intracellular copper sensors as we have previously (Bastos et al., 2018; Kasemets et al., 2009) because that approach does not enable membrane localisation to be assessed. Instead we used ToF-SIMS, where individual bacterial cells were first identified using K^+ mapping and copper was directly analysed with a combined ^{63}Cu + ^{65}Cu signal (Blockhuys et al., 2018). Following exposure to 12.5 mg/L copper, *i.e.* non-precipitating conditions in the bacterial medium, the copper signal was low at the bacterial cell membrane, the site of which was determined by $C_5H_{15}PNO_4^+$ as before (Nygren et al., 2007), and, was high intracellularly (Fig. 4). Collectively, our findings show that regardless of size, charge and composition of copper-based particles, it is the release of copper ions into solution that primarily determines their antimicrobial activity when aquated.

4. Discussion

It is well recognised that soluble forms of copper have antibacterial activity. However, whether particulate copper in suspension also has a

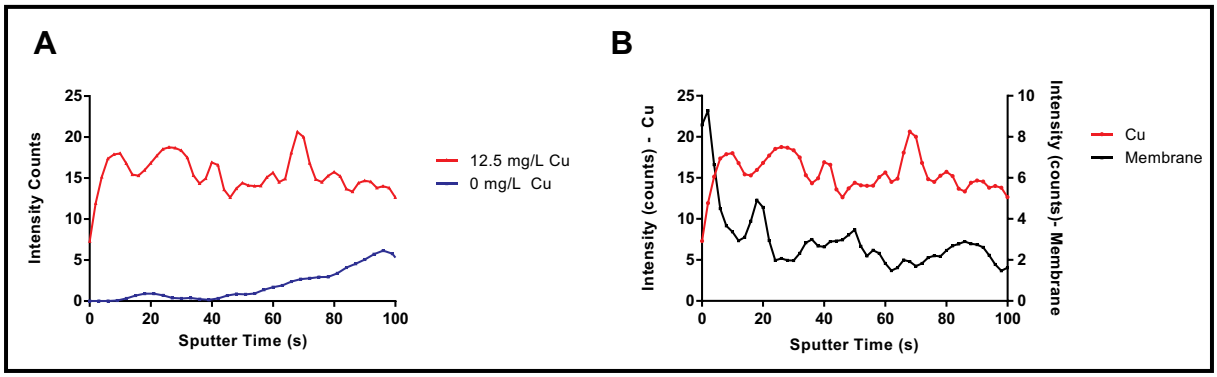

Fig. 4. Copper mapping in bacteria using Time-of-Flight Secondary Ion Mass Spectrometry (ToF-SIMS). (A) Depth profile for combined $^{63}Cu^+$, $^{65}Cu^+$ signal as a function of sputter time in samples where bacteria were exposed to 0 or 12.5 mg/L copper chloride; (B) and comparison between copper (combined $^{63}Cu^+$, $^{65}Cu^+$) and a membrane marker ($C_5H_{15}PNO_4^+$).

direct impact has not been established. Plausibility for this is posited on the fact that copper surfaces can be used to facilitate environmental infection control. Moreover, particles in suspension are, generally, attracted to cell membranes due to entropic and, often, electrostatic forces. Indeed, attractive forces could be enhanced using particle surface coatings although these then increase particle size, which is especially noticeable for the ultra small particle size range. On this point, it is unlikely that bacteria acquire and internalise ultra small (or larger) nanoparticles as the rigidity of the bacterial cell wall does not support endocytic mechanisms (Santos et al., 2018). Particle penetration could occur if the cell membrane was degraded by a specific particle coating or carrier (*e.g.* surfactants), but this would not be a direct nanoparticle interaction (Li et al., 2015; Xiu et al., 2012).

Here we show that, in the absence of a permeabilising agent, neither large nor small particles of copper-based materials have a measurable impact on bacterial growth above and beyond the effect through loss of copper ions into the aqueous medium. In other words, it is the dissolution of copper-based particles, but not their particulate nature *per se* that is responsible for the antimicrobial activity. Precisely what soluble products are formed and at what rates this occurs, will depend upon the particle itself as well as the nature of the aqueous environment. In the media used in this work (HMM) there are no strong chelating agents, but the presence of amino acids probably allows more copper in solution through weak moderate interactions with the metal, than water alone would allow. In other words, low molecular weight ligands can retard oxo-hydroxide formation of hydrolytic metal ions (such as copper) at near-neutral pHs. However, in this work, the same medium was used for all experiments, so conditions were matched except for particle type. As a result, concentration of soluble copper, over time, is the only variable that needed to be considered and its fractionation allowed robust modelling of the phase of copper that mediated the antimicrobial effect. Of course, we cannot exclude some effect of particulate copper-based material in terms of antimicrobial impact but this will be negligible compared to the soluble effect.

5. Conclusion

Apart from clarifying a rather long-standing question in the field, our findings have implications for both inadvertent and purposeful exposures to copper-based materials. For the former, it is likely that toxicity of copper-based materials to symbiotic bacteria is driven by solubility in an aqueous environment. For the latter, novel copper-based antimicrobial therapeutics should focus towards soluble rather than nanoparticulate forms of copper as antimicrobial actives. As noted above, nanosizing or other particulate structuring of copper materials may have advantage for delivery and formulation purposes, but we conclude that this is not the case for activity purposes, and, for which dissolution is the key.

Declaration of competing interest

The authors declare no conflict of interest but C.A.P.B., N.F., and J.J.P. wish to note that they are inventors on a patent detailing use of copper oxo-hydroxide structures as antimicrobials.

Acknowledgements

This work was supported by the University of Cambridge (UK) and funded by the UK Medical Research Council grant number MR/R005699/1.

Appendices. Supplementary Information

Supplementary data to this article can be found online at https://doi.org/10.1016/j.impact.2019.100192.

References

Aruoja, V., Dubourguier, H.-C., Kasemets, K., Kahru, A., 2009. Toxicity of nanoparticles of CuO, ZnO and TiO2 to microalgae *Pseudokirchneriella subcapitata*. Sci. Total Environ. 407, 1461–1468. https://doi.org/10.1016/j.scitotenv.2008.10.053.

Bastos, C.A.P., Faria, N., Ivask, A., Bondarenko, O.M., Kahru, A., Powell, J., 2018. Ligand-doped copper oxo-hydroxide nanoparticles are effective antimicrobials. Nanoscale Res. Lett. 13, 111. https://doi.org/10.1186/s11671-018-2520-7.

Bhattacharjee, S., 2016. DLS and zeta potential – what they are and what they are not? J. Control. Release 235, 337–351. https://doi.org/10.1016/j.jconrel.2016.06.017.

Blockhuys, S., Malmberg, P., Wittung-Stafshede, P., 2018. Copper distribution in breast cancer cells detected by time-of-flight secondary ion mass spectrometry with delayed extraction methodology. Biointerphases 13. In: 06E412, . https://doi.org/10.1116/1.5053814.

Cassini, A., Högberg, L.D., Plachouras, D., Quattrocchi, A., Hoxha, A., Simonsen, G.S., Colomb-Cotinat, M., Kretzschmar, M.E., Devleesschauwer, B., Cecchini, M., Ouakrim, D.A., Oliveira, T.C., Struelens, M.J., Suetens, C., Monnet, D.L., Group, B. of A.M.R.C, 2019. Attributable deaths and disability-adjusted life-years caused by infections with antibiotic-resistant bacteria in the EU and the European Economic Area in 2015: a population-level modelling analysis. Lancet Infect. Dis. 19, 56–66. https://doi.org/10.1016/S1473-3099(18)30605-4.

Chen, M., Qin, X., Zeng, G., 2017. Biodiversity change behind wide applications of nanomaterials? Nano Today 17, 11–13. https://doi.org/10.1016/j.nantod.2017.09.001.

Chen, J., Mao, S., Xu, Z., Ding, W., 2019. Various antibacterial mechanisms of biosynthesized copper oxide nanoparticles against soilborne *Ralstonia solanacearum*. RSC Adv. 9, 3788–3799. https://doi.org/10.1039/c8ra09186b.

EFSA, 2009. European Food Safety Authority (EFSA). Guidance of the scientific committee on use of the benchmark dose approach in risk assessment. EFSA J. 1150, 42–43. https://doi.org/10.2903/j.efsa.2009.1150.

EFSA, 2017. European Food Safety Authority (EFSA). Update: guidance on the use of the benchmark dose approach in risk assessment. EFSA J. 4658, 34–35.

EFSA, 2018. European Food Safety Authority (EFSA). Guidance on risk assessment of the application of nanoscience and nanotechnologies in the food and feed chain: Part 1, human and animal health. EFSA J. https://doi.org/10.2903/j.efsa.2018.5327.

ESCMID, 2003. Determination of minimum inhibitory concentrations (MICs) of antibacterial agents by broth dilution, by European Committee for Antimicrobial Susceptibility Testing (EUCAST) of the European Society of Clinical Microbiology and Infectious Diseases. Clin. Microbiol. Infect. 9, ix–xv. https://doi.org/10.1046/j.1469-0691.2003.00790.x.

Herrmann, H., Bucksch, H., 2015. Copper compound. In: Dictionary Geotechnical Engineering/Wörterbuch GeoTechnik, . https://doi.org/10.1007/978-3-642-41714-6_34811.

Ingle, A.P., Duran, N., Rai, M., 2014. Bioactivity, mechanism of action, and cytotoxicity of copper-based nanoparticles: a review. Appl. Microbiol. Biotechnol. 98, 1001–1009. https://doi.org/10.1007/s00253-013-5422-8.

Kasemets, K., Ivask, A., Dubourguier, H.-C., Kahru, A., 2009. Toxicity of nanoparticles of ZnO, CuO and TiO2 to yeast *Saccharomyces cerevisiae*. Toxicol. in Vitro 23, 1116–1122. https://doi.org/10.1016/j.tiv.2009.05.015.

LaRossa, R.A., Smulski, D.R., Van Dyk, T.K., 1995. Interaction of lead nitrate and cadmium chloride with *Escherichia coli* K-12 and *Salmonella typhimurium* global regulatory mutants. J. Ind. Microbiol. 14, 252–258. https://doi.org/10.1007/BF01569936.

Lemire, J.A., Harrison, J.J., Turner, R.J., 2013. Antimicrobial activity of metals: mechanisms, molecular targets and applications. Nat. Rev. Microbiol. 11, 371. https://doi.org/10.1038/nrmicro3028.

Li, H., Chen, Q., Zhao, J., Urmila, K., 2015. Enhancing the antimicrobial activity of natural extraction using the synthetic ultrasmall metal nanoparticles. Sci. Rep. 5, 11033. https://doi.org/10.1038/srep11033.

Malvern Instruments, 2015. Malvern Instruments Ltd - A Basic Guide to Particle Characterization.

McClements, D.J., Xiao, H., 2017. Is nano safe in foods? Establishing the factors impacting the gastrointestinal fate and toxicity of organic and inorganic food-grade nanoparticles. npj Sci. Food 1, 6. https://doi.org/10.1038/s41538-017-0005-1.

Moschini, E., Gualtieri, M., Colombo, M., Fascio, U., Camatini, M., Mantecca, P., 2013. The modality of cell–particle interactions drives the toxicity of nanosized CuO and TiO2 in human alveolar epithelial cells. Toxicol. Lett. 222, 102–116. https://doi.org/10.1016/j.toxlet.2013.07.019.

Nygren, H., Hagenhoff, B., Malmberg, P., Nilsson, M., Richter, K., 2007. Bioimaging TOF-SIMS: high resolution 3D imaging of single cells. Microsc. Res. Tech. 70, 969–974. https://doi.org/10.1002/jemt.20502.

Paulson, A.J., Kester, D.R., 1980. Copper(II) ion hydrolysis in aqueous solution. J. Solut. Chem. 9, 269–277. https://doi.org/10.1007/BF00644552.

Pfeiffer, C., Rehbock, C., Hühn, D., Carrillo-Carrion, C., de Aberasturi, D.J., Merk, V., Barcikowski, S., Parak, W.J., 2014. Interaction of colloidal nanoparticles with their local environment: the (ionic) nanoenvironment around nanoparticles is different from bulk and determines the physico-chemical properties of the nanoparticles. J. R. Soc. Interface 11, 20130931. https://doi.org/10.1098/rsif.2013.0931.

Raffi, M., Mehrwan, S., Bhatti, T.M., Akhter, J.I., Hameed, A., Yawar, W., ul Hasan, M.M., 2010. Investigations into the antibacterial behavior of copper nanoparticles against *Escherichia coli*. Ann. Microbiol. 60, 75–80. https://doi.org/10.1007/s13213-010-0015-6.

Reller, L.B., Weinstein, M., Jorgensen, J.H., Ferraro, M.J., 2009. Antimicrobial susceptibility testing: a review of general principles and contemporary practices. Clin. Infect. Dis. 49, 1749–1755. https://doi.org/10.1086/647952.

Santos, R.S., Figueiredo, C., Azevedo, N.F., Braeckmans, K., De Smedt, S.C., 2018. Nanomaterials and molecular transporters to overcome the bacterial envelope barrier: towards advanced delivery of antibiotics. Adv. Drug Deliv. Rev. 136–137, 28–48. https://doi.org/10.1016/j.addr.2017.12.010.

Sarkar, R.K., Chattopadhyay, A.P., Aich, P., Chakraborty, R., Chatterjee, A.K., Basu, T., 2012. A simple robust method for synthesis of metallic copper nanoparticles of high antibacterial potency against *E. coli*. Nanotechnology 23.

Wills, J.W., Johnson, G.E., Doak, S.H., Soeteman-Hernández, L.G., Slob, W., White, P.A., 2015. Empirical analysis of BMD metrics in genetic toxicology part I: in vitro analyses to provide robust potency rankings and support MOA determinations. Mutagenesis 31, 255–263. https://doi.org/10.1093/mutage/gev085.

Wills, J.W., Long, A.S., Johnson, G.E., Bemis, J.C., Dertinger, S.D., Slob, W., White, P.A., 2016. Empirical analysis of BMD metrics in genetic toxicology part II: in vivo potency comparisons to promote reductions in the use of experimental animals for genetic toxicity assessment. Mutagenesis 31, 265–275. https://doi.org/10.1093/mutage/gew009.

Wills, J.W., Summers, H.D., Hondow, N., Sooresh, A., Meissner, K.E., White, P.A., Rees, P., Brown, A., Doak, S.H., 2017. Characterizing nanoparticles in biological matrices: tipping points in agglomeration state and cellular delivery in vitro. ACS Nano 11, 11986–12000. https://doi.org/10.1021/acsnano.7b03708.

Xiu, Z., Zhang, Q., Puppala, H.L., Colvin, V.L., Alvarez, P.J.J., 2012. Negligible particle-specific antibacterial activity of silver nanoparticles. Nano Lett. 12, 4271–4275. https://doi.org/10.1021/nl301934w.

Zhang, J., Richardson, H.W., 2016. Copper Compounds. In: Ullmann's Encyclopedia of Industrial Chemistry. American Cancer Society, pp. 1–31. https://doi.org/10.1002/14356007.a07_567.pub2.